Correction of the Photovoltaic System Control by the Addition of a Voltage Regulator in the Electrical Conversion Chain

Ali Ghelam[1*], Mohamed Boudiaf[2], Yazid Derouiche[3]
1- LAADI Laboratory, Ziane Achour University, Algeria.
Email: ghelam@gmail.com (Corresponding author)
2- LAADI Laboratory, Ziane Achour University, Algeria.
Email: boudhiaf_mohamed@yahoo.fr
3- Physics Department, Ziane Achour University, Algeria.
Email: yazidderouiche@gmail.com

Received: December 2019 Revised: April 2020 Accepted: June 2020

ABSTRACT:
The objective of this work is to meet the variations of the electrical energy needs by modifying the conventional topology of the conversion chain, at the same time to improve the operation of the photovoltaic system. This article focuses on improving the performance and efficiency of photovoltaic systems connected to the AC grid, through the use of advanced control algorithms (Sliding Mode control SMC and Fuzzy Logic Control FLC) for the control of DC/DC and DC/AC power conditioners. The control of the DC/DC converter allows the pursuit of the maximum power point MPPT of the photovoltaic generator with a view to a better utilization of the photovoltaic generator. The inverter control system is used to inject synchronized sinusoidal output current to the power grid and to improve the quality of energy injected into the grid. The original idea of this work is based on the insertion of a DC/DC BOOST voltage regulator in the conversion chain (between the battery and the inverter) to adjust the voltage transfer of the DC bus. This technique allows the provision of AC voltage for the sufficiency of the energy required by the control according to the need of the load.

KEYWORDS: Photovoltaic Conversion Chain, DC/DC Boost Converter, DC/AC Converter, Voltage Regulator, Power Regulation, MPPT, Fuzzy Logic Controller, Sliding Mode Control.

1. INTRODUCTION

Photovoltaic solar energy has been growing strongly in recent years because it is an inexhaustible source, non-polluting for the environment, silent and with a very low level of risk. With the increase in the price of fossil fuels, the exploitation of this resource with Photovoltaic Generation (PVG) systems becomes viable and profitable. It is available during peak energy periods, unlike the wind, which often produces more energy at night than during the day. Solar or photovoltaic panels are the basic element of any photovoltaic system. They consist of photosensitive cells connected to each other [1]. Each cell converts the rays coming from the sun into electricity thanks to the photovoltaic effect. Photovoltaic panels have a specific electrical characteristic that is given by the manufacturer in the form of curves. These curves generally represent the evolution of the current and the power with respect to the voltage of the panel. The electrical characteristic of the panel is of a nonlinear nature and has a particular point called "Maximum Power Point" (MPP). This point is the optimum operating point for which the panel operates at its maximum power [2].

The optimization of the photovoltaic energy production is generally obtained by ensuring a good adaptation between the PV generator and the associated receiver. This adaptation is carried out using a BOOST DC/DC static converter controlled by the MPPT control technique and a DC/AC converter for connecting the energy to the AC network in the various operating modes [3].

It is necessary to equip the autonomous or non-autonomous photovoltaic systems with accumulator batteries which makes it possible to store the energy and to restore it in due time, in spite of the availability of these batteries, the energy supplied to the load remains sometimes insufficient (in the case where the energy demanded is very strong), is this due to the design of the photovoltaic systems used which we have thought of a solution to this problem, then the proposed solution is

Doi: https://doi.org/10.29252/mjee.14.3.5
How to cite this paper: A. Ghelam, M. Boudiaf, and Y. Derouiche, **“Correction of the Photovoltaic System Control by the Addition of a Voltage Regulator in the Electrical Conversion Chain”**, *Majlesi Journal of Electrical Engineering*, Vol.14, No. 3, pp. 45-52, 2020.

the insertion of a Voltage regulator type DC/DC BOOST between the battery and the inverter, it leads *to* the modification of the electrical conversion circuit used.

In this work, we present the simulation of new conversion topology (With insertion of a DC/DC BOOST voltage regulator) in comparison with the conventional conversion topology (without voltage regulator). In this new topology, we introduce Fuzzy Logic control (FLC) and Sliding Mode Control (SMC) for the regulation of the electrical conversion chain. Our application is based on the development and improvement of the coupling part to the alternative network.

2. STRUCTURE OF THE STUDIED SYSTEM

Figs. 1 and 2 show successively the two conversion topologies used in this work, such as: the ordinary version (classic) and the improved version (as an original idea).

In Fig. 1, the GPV is connected to the AC network via a DC/DC BOOST converter controlled in MPPT and a DC/AC power-controlled converter (This inverter is coupled to the AC network by a coupling transformer T).

The second topology (Fig. 2), shows the same structure of version 1 with a modification by the insertion of a voltage regulator converter in cascade with the inverter.

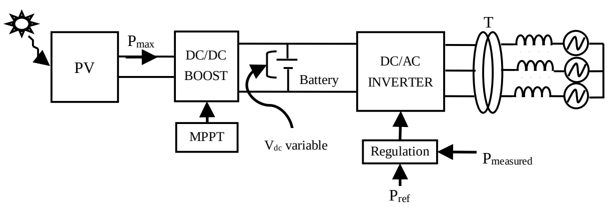

Fig. 1. Ordinary topology (version 1).

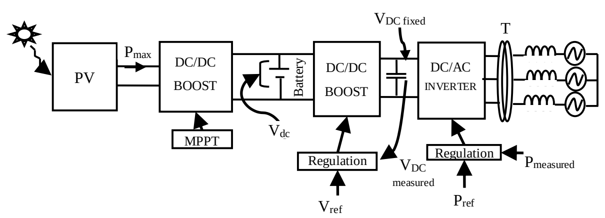

Fig. 2. Improved topology (version 2).

3. PROBLEMATIC

To solve the problem of insufficient DC voltage on the inverter as part of the power control strategy, we have two solutions.

- 1st solution: Inserting more batteries → this is a very expensive solution that requires a lot of maintenance and a lot of space (Fig. 3).

- 2nd solution: Inserting a DC-DC BOOST voltage regulator → it is a less expensive solution which requires less maintenance, allows supplying the inverter with a fixed DC voltage until the total discharge of the battery (Fig. 4).

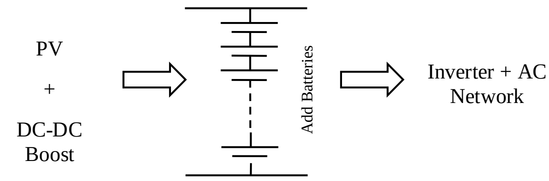

Fig. 3. Insert more batteries.

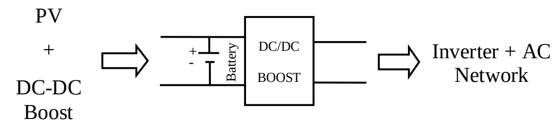

Fig. 4. Insertion of DC-DC voltage regulator.

The following Figs. 5 and 6 show the effect of a voltage regulator converter for changing the amplification gain of the inverter. Note in Fig. 5, the amplification gain of the inverter $G_0=V_{dc}/(2V_p)$. The insertion of a voltage regulator (C) makes it possible to modify G_0 to a new value $G=C*G_0$ to increase the maximum efficiency of the control circuit and to ensure the regulation under the higher-order conditions of the load (Fig. 6).

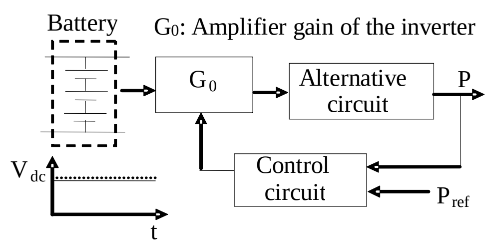

(V_{dc}: DC Voltage, V_p: Triangular signal amplitude of PWM control)

Fig. 5. Classical model $G_0=V_{dc}/(2V_p)$.

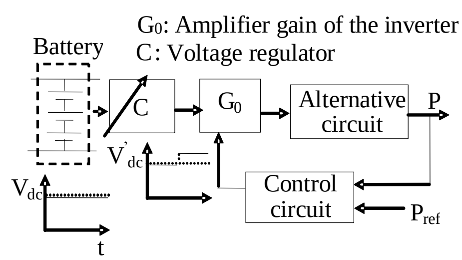

$G=C*G_0=C*V_{dc}/(2V_p)$ and $V'_{dc}=C*V_{dc}$

Fig. 6. Modified model.

4. FUNCTIONING AND MODELING OF THE STUDIED SYSTEM

4.1. Modeling of the DC/DC Converter (Boost)

To obtain a better efficiency of the electrical energy produced from the solar energy received from a photovoltaic installation, it is necessary to use a DC-DC converter (chopper) making it possible to operate the PV module at its optimum power. We use for this:

- A DC/DC converter Boost (Version 1) with MPPT (Maximum Power Point Tracking) control for the search of the Maximum Power Point allowing the PV panel to operate at optimum power.

- A DC/DC Boost- voltage regulator (Version 2) to fix the DC bus voltage at the inverter terminal against variations due to the change of the requested power and the variation of the energy produced by the generator photovoltaic because of climate change.

Fig. 7 shows the structure of a BOOST DC/DC converter placed between the photovoltaic generator and the DC/AC converter (inverter) controlled by its duty cycle “d” [4-6]. The MPPT control structure (for boost1) or the DC voltage control (for boost2) allows adjusting the duty cycle to follow the chosen setpoint at any time.

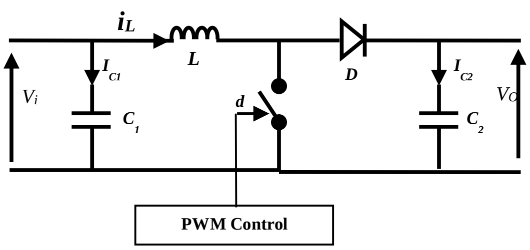

Fig.7. Structure of a DC/DC Boost Converter

The ratio of the output voltage to the input voltage of the DC/DC boost converter in continuous mode is given by the following relation:

$$\frac{V_O}{V_i} = \frac{1}{1-d} \quad (1)$$

Equations (2) describe the modeling of the DC-DC BOOST converter in all phases of operation (d: the duty cycle).

$$\begin{bmatrix} \dfrac{dv_o}{dt} \\ \dfrac{di_L}{dt} \end{bmatrix} = \begin{bmatrix} -\dfrac{1}{R_0 C} & \dfrac{1-u}{C} \\ -\dfrac{1-u}{L} & 0 \end{bmatrix} . \begin{bmatrix} v_o \\ i_L \end{bmatrix} + \begin{bmatrix} 0 \\ \dfrac{1}{L} \end{bmatrix} V_i \quad (2)$$

R₀: Load resistance;
u: Signal Control;

4.2. Modeling of the DC/AC Converter (inverter)

An inverter is a static converter that converts electrical energy from the continuous form (DC) to the alternative form (AC). In fact, this energy conversion is satisfied by means of a control device (semiconductors). It allows obtaining receiver terminals at an alternating voltage adjustable in frequency and in effective value, in thus using an adequate command sequence [7-8], Fig. 8 shows the electrical structure of a three-phase inverter.

The inverters consist of dimensioned active and passive components which nevertheless admit a certain number of limitations which are not without consequences on the synthesis of the control loop.

The use of power MOSFETs will be put forward to allow for a higher switching frequency. On the other hand, a compromise will have to be made since a higher switching frequency implies greater switching losses and the heating of the various components constitute this inverter and thus a decrease in the efficiency [9].

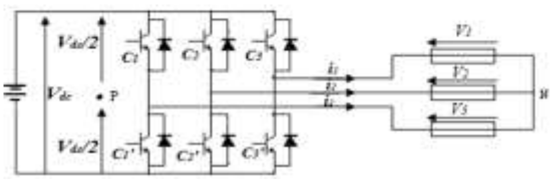

Fig. 8. Electrical structure of a three-phase inverter with two levels.

In our work, the PWM control strategy is used to generate the switching signals.

Equations (3) and (4) describe the conversion model of the two-level DC/AC inverter used;

$$\begin{bmatrix} V_a \\ V_b \\ V_c \end{bmatrix} = V_{DC} . \begin{bmatrix} 2/3 & -1/3 & -1/3 \\ -1/3 & 2/3 & -1/3 \\ -1/3 & -1/3 & 2/3 \end{bmatrix} . \begin{bmatrix} c_a \\ c_b \\ c_c \end{bmatrix} \quad (3)$$

$$I_{DC} = c_a i_a + c_b i_b + c_c i_c = [c_{abc}]^T . [i_{abc}] \quad (4)$$

V_{DC}: DC voltage, I_{DC}: DC current, V_a, V_b, V_c; The three-phase output voltages of the converter and C_a, C_b, C_c: Switching signals generated by the PWM control strategy.

5. CONVERTER CONTROL STRATEGY

5.1. Regulatory Diagrams

Figs. 9, 10 and 11 respectively show the control diagrams of two DC-DC BOOST converters and a DC-AC inverter.

We use :

- The MPPT (Perturbed & Obserbed: P & O) control for regulating the first DC-DC BOOST in the output of the solar panel;

- The control by Fuzzy Logic Controller (FLC) for the conditioning of second DC-DC BOOST voltage regulator between the battery and the inverter;

- The Sliding Mode Control (SMC) command in cascade with the FLC command for the regulation of the DC-AC converter (the inverter).

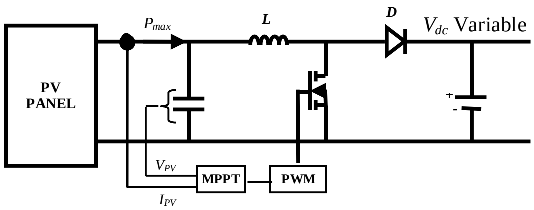

Fig. 9. MPPT control.

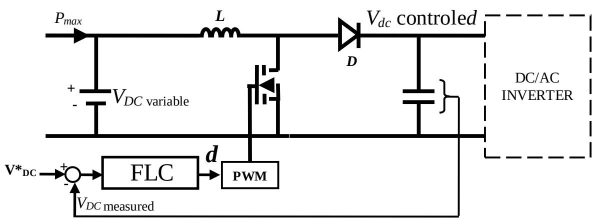

Fig.10. FLC regulation of DC-DC BOOST voltage Regulator.

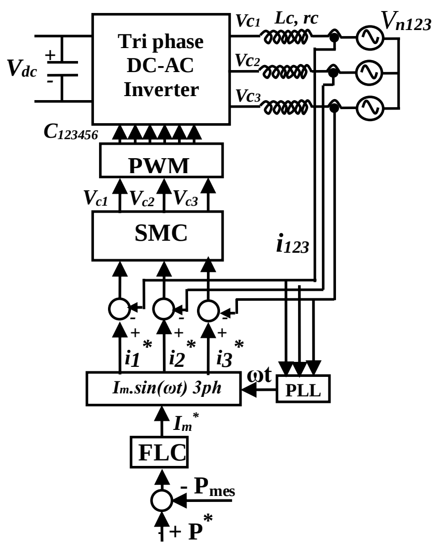

Fig. 11. SMC regulation in cascade with the FLC regulation of DC/AC Inverter.

The MPPT command always intervenes to optimize the efficiency of the PV generator by determining a cyclic ratio coincided with the maximum power.

However, in the DC/DC converter BOOST voltage regulator the duty cycle is generated by the Fuzzy Logic Regulator (FLC) to control the DC output voltage V_0 [10] (Fig.10). In Fig.11, there is a fuzzy logic controller for generating reference current amplitude I_m* for setting the active power and a stage for three Sliding Mode Controller (SMC) for setting three-phase currents generated by the converter to the AC network. To calculate the three reference three-phase currents, a PLL block and a calculation methodology are used.

5.2. Regulatory Strategies

The diagram of the following Fig. 12 shows the detail of the MPPT (P&O) technique used to synthesize the 1st DC-DC BOOST converter: This method is used to improve the efficiency of the PV system. [11]

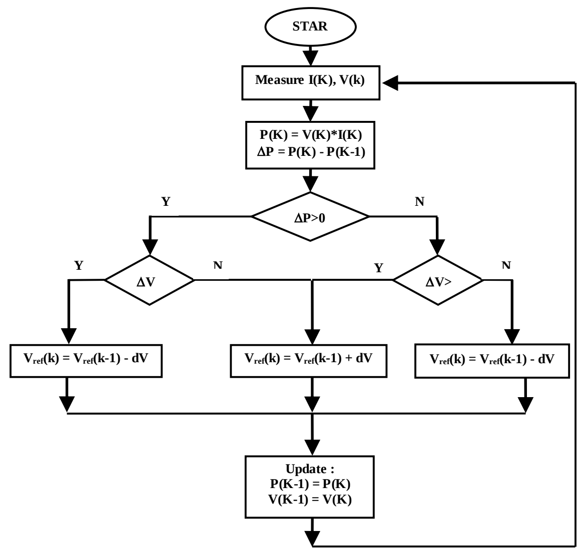

Fig.12. MPPT Algorithm by P&O

Fig. 13 shows the current regulation block diagram provided by the inverter to the AC grid (for phase ***1***): The Sliding Mode Control (SMC) control strategy is used [12-15].

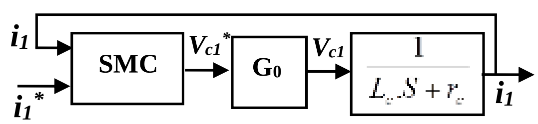

Fig. 13. Sliding mode control scheme.

By putting $x_k = i_k$ and $x_k^* = i_k^*$ (k= 1,2,3), we obtain the following model:

$$\dot{x}_k = \frac{1}{L_c}[(V_{ck} - V_{nk}) - r_c.x_k] \qquad (5)$$

By taking as a sliding surface $S = e$, we obtain

$$\dot{S}_k = \dot{x}_k^* - \dot{x}_k \qquad (6)$$

The condition $S.\dot{S} < 0$ ensures the attractiveness of the trajectory towards the sliding surface. To do this, simply choose the command such as:

$$V_{ck}^{*} = \frac{1}{G_0}[V_{nk} + BL_c sign(e_k) + L_c \dot{x}_k^{*} + r_c x_k] \qquad (7)$$

G_0: DC/AC converter gain, B: Coefficient of regulation.

Following the complexity and nonlinearity of the DC-DC converter model and the active power model injected by the DC-AC converter and the equipment with a wide range of operation; it is plausible to think on a control strategy that could be based on a model-free approach. To handle the subjectivity associated with the inexact nature of the studied model, one can use a PI fuzzy logic controller [16-18].

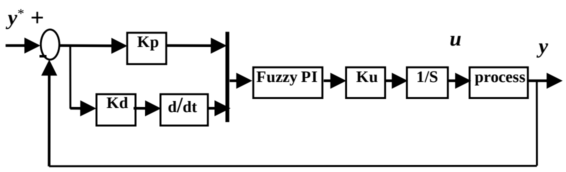

Fig.14. Fuzzy PI Controller.

Y = p (Injected power) and ***u***=I^*_m (Injected current) for the active power control loop at the inverter (Fig.15.a).

y = Vo (Output Voltage) and ***u=d*** (duty cycle) for the DC-DC converter BOOST Voltage regulator (Fig.15.b).

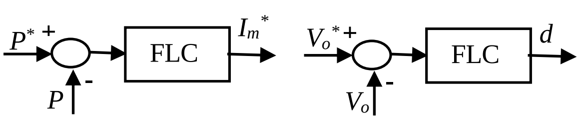

(a) (b)

Fig. 15. FLC Application.

In the fuzzification stage of PI fuzzy controller, error ***e*** and error variation ***de*** are the controller inputs. The number of input membership functions used in input scaling are three: ***N*** (negative), ***P*** (positive) and ***Z*** (zero) as shown in Fig. 16.

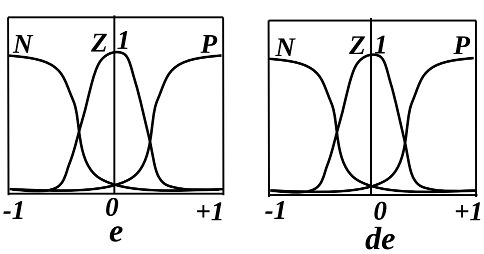

Fig.16. Membership function of ***e*** and ***de.***

The output membership functions for fuzzy logic controller are selected as shown in Fig. 16

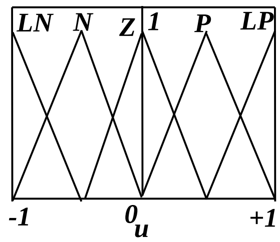

Fig. 17. Membership function of ***u*** (***u*= *d*** or I_m^*).

The five linguistic variables used for error and error variations are:

LN: large negative, ***N***: negative, ***Z***: zero, ***P***: positive, ***LP***: large positive.

Table 1. The fuzzy rules used.

de \ *e*	*N*	*Z*	*P*
N	***LP***	***P***	***Z***
Z	***P***	***Z***	***N***
P	***Z***	***N***	***LN***

To convert the fuzzy sets to the real numbers, the centroid defuzzifier is used to calculate the output change ***d*** of the fuzzy PI controller.

$$\boldsymbol{d} = \frac{\sum_{i=1}^{n} h_i u_i}{\sum_{i=1}^{n} u_i} \qquad (8)$$

u_i is the its membership function and h_i is its center.

6. SIMULATION RESULTS

Here we present the simulation results to illustrate the regulatory performance of the new model in deciding to use this circuit modification in the next photovoltaic installations. The comparative simulation of two control configurations (version 1 (a) and version 2 (b)) using three control strategies (MPPT, FLC and SMC) on the three conversion circuits of the PV chain makes it possible to obtain the following results:

Figs. 18.a and 18.b below show the control behavior of active power injected into the alternative network in the two proposed versions. For Fig. 18.a, note an unacceptable static error from 0.2 sec (the moment of increase in power demand). But for Fig. 18.b, there is a zero static error in best setpoint tracking during the entire control period (which explains the effectiveness of the new version proposed to meet the power demand).

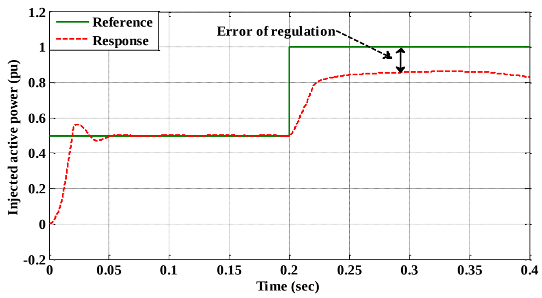

(a) Version 1 (Ordinary)

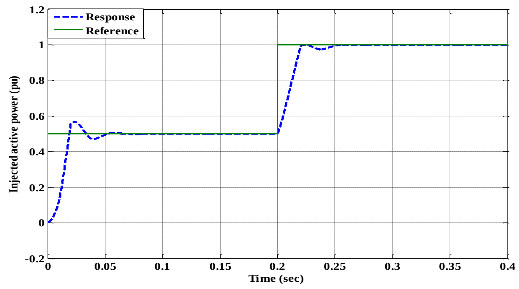

(b) Version 2 (Modified)

Fig. 18. Injected active power.

Fig.19a and Fig.19b show successively the regulation of the alternating current injected into the electrical network for the two versions (1) and (2). In Fig. 19.a, we notice the total degradation of the command with no setpoint tracking and the reference divergence. By cons in Fig. 19.b, we note that the current follow the order of the command.

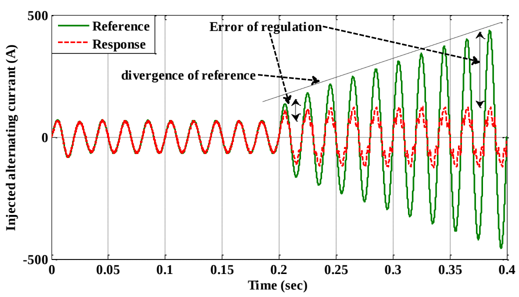

(a) Version 1 (Ordinary)

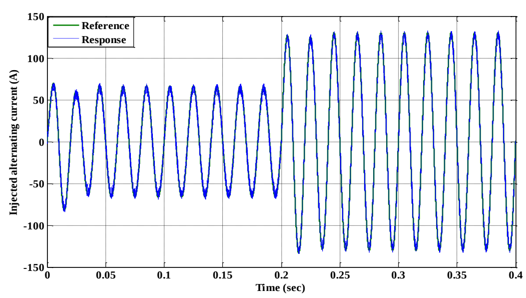

(b) Version 2 (Modified)

Fig. 19. Injected alternating current.

On the following Fig. 20 (the zoom of Fig. 19.b), we find that the injected alternating current follow the reference current with a better quality of the signal.

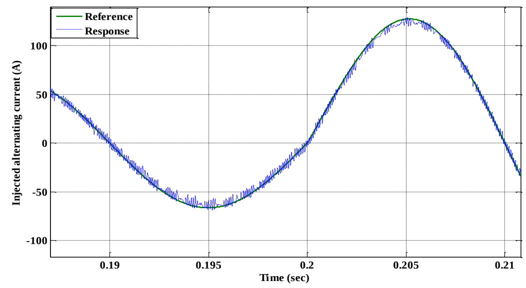

Fig. 20. Zoom of the previous Fig. 19.b (Modified version)

Fig. 21.a and 21.b show the variation of the direct current absorbed by the DC-AC converter (inverter) in the two configurations used. We observe that the average value of the current in the 2nd version (new) is lower than that of the 1st (ordinary) throughout the duration of regulation. The quality of the 2nd version signal is more optimized compared to the 1st.

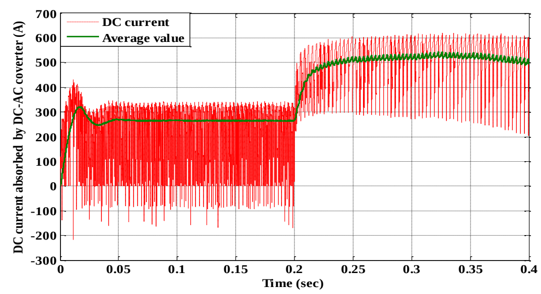

(a) Version 1 (Ordinary)

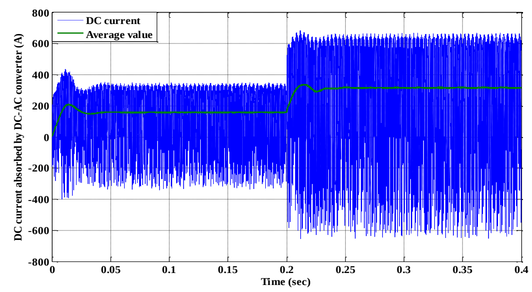

(b) Version 2 (Modified)

Fig. 21. DC current absorbed by DC-AC converter.

Note in Fig.22.a, the decrease and degradation of the input voltage quality of the inverter, in contrast in Fig. 22.b, the voltage regulator intervenes to make the voltage continues to always follow the order with small disturbances in the instants of change of active power setpoint injected into the AC network.

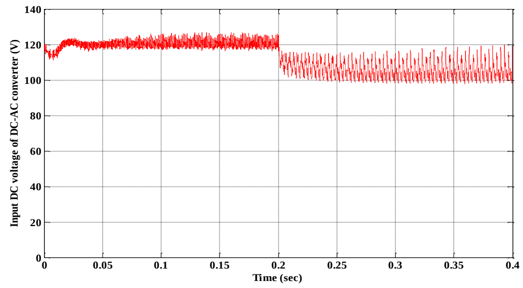

(a) Version 1 (Ordinary)

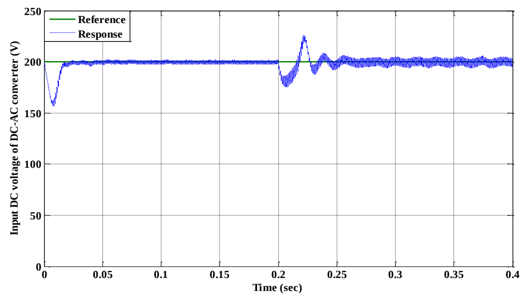

(b) Version 2 (Modified)

Fig. 22. Input DC voltage of DC-AC converter.

The MPPT command forces the PV generator to provide maximum power during the regulation period (before and after 0.2 sec) in both versions. Except for a slight disturbance, at the moment 0.2sec (Fig. 23.b) because of the strong variation in absorption of direct current in the sense of the voltage regulator.

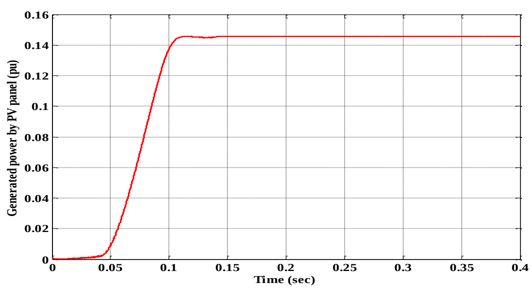

(a) Version 1 (Ordinary)

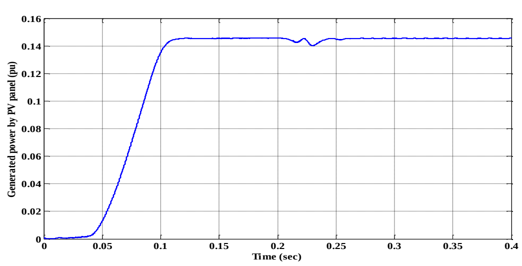

(b) Version 2 (Modified)

Fig. 23. Generated power by the PV panel.

Figs. 24 and 25 show successively the variation of the electrical characteristics (current **-** voltage) provided by the storage battery. There is a significant increase in the current and a considerable decrease in voltage after 0.2 sec (the moment of energetic variation).

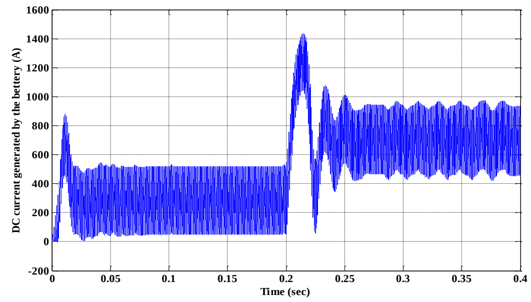

Fig. 24. DC current generated by the battery Version 2 (Modified).

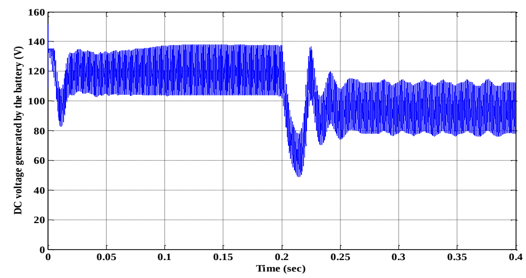

Fig. 25. DC voltage generated by the battery Version 2 (Modified).

7. CONCLUSION

The technical importance of integrating the DC voltage regulator in photovoltaic systems has become essential to adapt the load to the photovoltaic panel and to condition the shape of the energy according to the limiting conditions in all elements of the electrical conversion chain. The 1st model (ordinary version) does not satisfy the power demanded by the load in case of high consumption despite the use of advanced control strategies (FLC and SMC). Based on the advantage of high performance for active power and alternating current control using the new modification of the conversion chain by adding the 2nd DC-DC voltage regulator converter (as an original work) in comparison with the former model (ordinary), we conclude that the use of this new structure allows to meet the requirements of the load variation in the max conditions and allows to supply the inverter by the DC voltage necessary according to the needs of the order without influence on the characteristics of the 1st DC-DC converter in MPPT.

In other ways, this method can correct the amplification gain of the DC-AC converter. In some cases in parallel with the use of advance control strategies, it is necessary to modify the electrical circuit to push the responses towards the desired values. In addition, our results give an addition to the photovoltaic industry to advance more and more.

8. APPENDIX

The alternative network: $L_c=0.02H$, $r_c=0.5\Omega$, $V_n=230$, $f=50Hz$.
The transformer ratio associated with the inverter $N_T = 10$.
The DC-DC converter BOOST: L=0.01H, C=2μF.
Base power $P_B=50KW$.
Coefficient of regulation for (SMC): $B=100$.
The adaptation gains of the fuzzy logic controller:
$Kp=0.01$, $Kd=10$, $Ku=2$.

REFERENCES

[1] Xenophontos, A., & Bazzi, A. M. **"Model-Based Maximum Power Curves of Solar Photovoltaic Panels Under Partial Shading Conditions".** *IEEE Journal of Photovoltaics*, Vol. 8(1), 233-238, 2018.

[2] Hassan, A., Dash, A., & De, D. **"Comparison of converter structures for residential PV system with module based maximum power point tracking".** *Technologies for Smart-City Energy Security and Power (ICSESP*), 2018.

[3] Ruiz-Cortes, M., Gonzalez Romera, E., Amaral Lopes, R., Romero-Cadaval, E., Martins, J., Milanes Montero, M. I., & Barrero, F. **"Optimal Charge/Discharge Scheduling of Batteries in Microgrids of Prosumers".** *IEEE Transactions on Energy Conversion*, pp. 1-1, 2018.

[4] Pandey, S. K., Patil, S. L., & Phadke, S. B. **"Comment on "PWM-Based Adaptive Sliding-Mode Control for Boost DC-DC Converters"** [Aug 13 3291-3294]. *IEEE Transactions on Industrial Electronics*, Vol. 65(6), pp. 5078-5080, 2018.

[5] Ikeda, S., & Kurokawa, F. **"Boost full bridge DC-DC converter ensuring safe installation of PV energy in data center power management systems",** 2017 *IEEE International Telecommunications Energy Conference (INTELEC*), 2017.

[6] Kar, R. R., & Aftab Alam, M. "**Design and Modeling of High Power DC-DC Boost Converter for Solar Photovoltaic System".** 2018 International Conference on Soft-*Computing and Network Security (ICSNS),* 2018.

[7] Jia, Q., Yan, G., Cai, Y., & Li, Y. **"Small signal stability analysis of paralleled inverters for multiple photovoltaic generation units connected to weak grid"**. *The Journal of Engineering*, Vol. 13, pp. 2015–2020, 2017.

[8] Ma, J., Zhao, D.-W., Qian, M.-H., Zhu, L.-Z., & Geng, H. **"Modelling and validating photovoltaic power inverter model for power system stability analysis",** *The Journal of Engineering*, Vol. 13, pp. 1605-1609, 2017.

[9] Kebir, A. E., Belhadj, H., Negadi, K., & Bey, A. B. **"Design and Construction of an Inverter for a Photovoltaic System".** *2018 IEEE XXVII International Scientific Conference Electronics – ET*, 2018.

[10] Hannan, M. A., Ghani, Z. A., Hoque, M. M., Jern, K. P., Hussain, A., & Mohamed, A. "**Fuzzy logic inverter controller in photovoltaic applications: Issues and recommendations"**. *IEEE Access*, pp. 1-1, 2019.

[11] Subudhi, B., & Pradhan, R. "**A New Adaptive Maximum Power Point Controller for a Photovoltaic System".** *IEEE Transactions on Sustainable Energy*, pp. 1-1, 2018.

[12] Safari , H. Ardi, **"Sliding Mode Control of a Bidirectional Buck/Boost DC-DC Converter with Constant Switching Frequency",** *Iranian Journal of Electrical and Electronic Engineering IJEEE*, Vol. 14, Issue 1, 2018.

[13] Houda LAABIDI, Houda JOUINI, Abdelkader MAMI, **" Sliding Mode Control for PV-Wind Hybrid System Connected to Grid",** *International Conference on Green Energy & Environmental Engineering (GEEE-2018), Proceeding of Engineering and technology-PET* , Vol. 37, pp. 39-44, 2018.

[14] Zhu, Y., & Fei, J. **"Adaptive Global Fast Terminal Sliding Mode Control of Grid-connected Photovoltaic System Using Fuzzy Neural Network Approach".** *IEEE Access*, Vol. 5, pp. 9476-9484, 2017.

[15] Zhao, T., Ji, N., Xu, H., & Zhang, T. **"Study on Variable Step Sliding-Mode Based MPPT for PV Array"**. *2019 14th IEEE Conference on Industrial Electronics and Applications (ICIEA*), 2019.

[16] KRISHNA NAICK, **"Fuzzy Logic Controller based PV System Connected in Standalone and Grid Connected Mode of Operation with Variation of Load"**, *International Journal of Renewable Energy Research-IJRER*, Vol. 7, No. 1 2017.

[17] Priya Kumari, Ashutosh Pandey, D. Sivakumar, S. Balaji, "**Fuzzy Logic based Battery Energy Storage System (Bess) for the Improvement in Stability of an Islanded Micro-Grid"**, *International Journal of Recent Technology and Engineering (IJRTE*), Vol. 8, Issue 1S4, 2019.

[18] Callegaro, L., Ciobotaru, M., Pagano, D. J., & Fletcher, J. E. **"Feedback Linearization Control in Photovoltaic Module Integrated Converters".** *IEEE Transactions on Power Electronics*, pp. 1–1, 2018.